Research Article

Heat Loss Analysis of Continuous Drying Oven with Outside Conveyor Chain

Weerayut Jitwiriya*, Tonkid Chantrasmi, Udomkiat Nontakaew and Pisit Yongyingsakthavorn
Department of Mechanical and Aerospace Engineering, Faculty of Engineering, King Mongkut's University of Technology North Bangkok, Bangkok, Thailand

* Corresponding author. E-mail: weerayut.j@cit.kmutnb.ac.th DOI: 10.14416/j.asep.2020.07.003
Received: 17 February 2020; Revised: 30 April 2020, Accepted: 26 June 2020; Published online: 21 July 2020

Abstract
In continuous manufacturing lines, conveyor chains are employed to transport future products in and out of these ovens in various processes of the production. As such, the typically metal conveyor system creates a significant heat loss by absorbing the thermal energy from inside the oven and releasing it outside. This work analyzed heat transfer of a novel drying oven design with their conveyor chains outside of the heated zone. The problem was complex due to multiple modes of heat transfer and an intermediate area between the heated zone and the outside chain. A mathematical model was proposed along with a numerical solution approach based on Finite Difference Method (FDM). Using problem parameters from a real latex-gloves production line as an example, it was found that the new design could reduce the heat loss by 23.1% when replacing all conventional ovens with the new designs.

Keywords: Drying oven, Energy analysis, Finite difference method

1 Introduction

Nowadays, many mass production manufacturing lines use closed-loop conveyor system to deliver the future products through various stages of the productions, possibly including many heated ovens. These ovens typically use a lot of thermal energy to reduce the moisture from the products. Reducing their heat consumption will give an advantage in term of production cost.

Defraeye [1] compiled the drying researches and development from 1985 to 2015. There was a clear trend of development to increase thermal efficiency to reduce the production cost in many industries. Radiation ovens were not very suitable for mass production lines, so hot-air convective technique or the combination was applied in many applications for higher efficiency. In Jitwiriya [2], a hot-air recirculation system was proposed to reduce the waste thermal energy by optimized recirculation ratio and drying temperature. Rattanapan [3] proposed using the eco-efficiency theory and material flow analysis to reduce the energy cost. Mathematical models of heat transfer of drying process were presented by many studies [4]–[6]. In addition, many works [7]–[11] proposed Conjugate Heat Transfer (CHT) models of convective drying process in order to analyze complex thermal behaviours.

Heat loss due to the conveyor system moving through the ovens remains one of the largest thermal waste in many manufacturing lines. Moreover, this causes thermal fatigue of the conveyor system as discussed in Fedorko *et al*. [12] and Elazayady *et al*. [13]. A good example of plants with this particular thermal waste is gloves manufacturing lines.

Recently, Yingyongsakthavorn *et al*. [14] proposed many changes to the traditional continuous latex-gloves production lines by introducing ideas and proofs of concepts such as a novel design for stripping machines, a new drying oven with outside chain (similar

Please cite this article as: W. Jitwiriya, T. Chantrasmi, U. Nontakaew, and P. Yongyingsakthavorn, "Heat loss analysis of continuous drying oven with outside conveyor chain," *Applied Science and Engineering Progress*, vol. 14, no. 3, pp. 387–396, Jul.–Sep. 2021, doi: 10.14416/j.asep.2020.07.003.

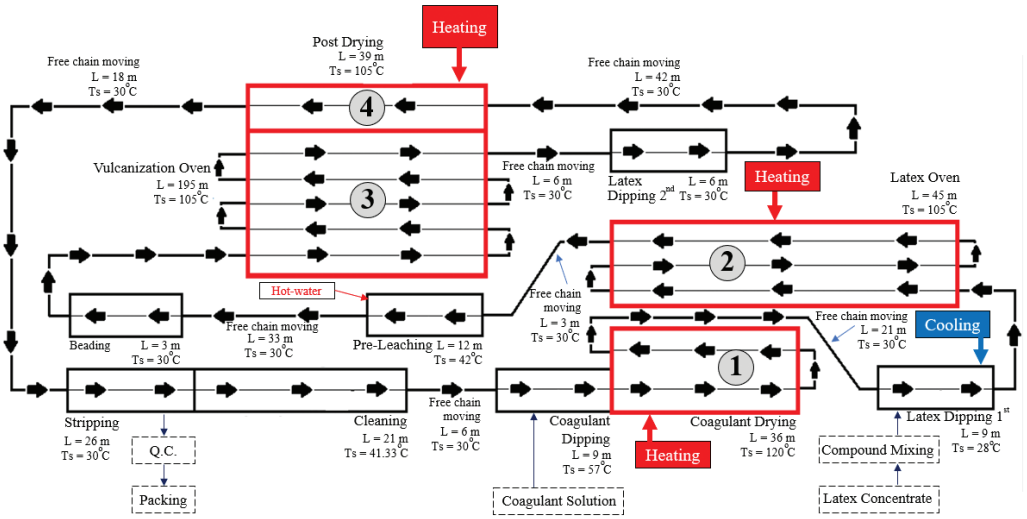

Figure 1: An example of latex-gloves production line with indicated temperature of each subprocess.

to the work presented here) and potential improvement on the vulcanization process.

Figure 1 shows an example of closed-loop continuous latex-gloves production lines. Air temperature and distance of each section of the entire production line are presented. The conveyor system carried the formers (molds) through 11 subprocesses – not including the "free chain" sections in-between – with conveyor speed of 0.3 m/s. In this example, there are four drying ovens: coagulant, latex, vulcanization and post-drying ovens. Since the conveyor system is moving through many different temperature ranges, the typically metal parts act as a carrier to absorb heat from the ovens to release outside. One proposed solution to reduce this thermal waste is to have as much of the conveyor system outside the heated region in the ovens as shown in Figure 2.

Figure 3 shows a more realistic design with some engineering. For sake of brevity, this oven design will be referred to in this work simply as "new oven design". Holder and former covers (air-barrier plates) are crucial to significantly reduce the leakage from the side gaps along the entire length of the oven. This side gap is unavoidable consequence of having the holders and conveyor chain outside of the heated region. When performing heat transfer analysis, one must consider the control volume between the heated region and the holder covers as another zone since the temperature inside this zone is different than the set oven temperature

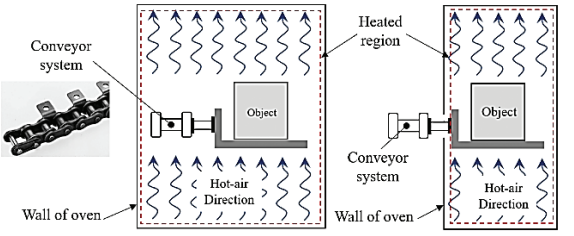

Figure 2: Comparing the conventional oven (left) to the new design with the conveyor system outside the heated region (right).

and the outside temperature.

In this research, a CHT model of the new oven design is formulated without considering humidity effects. In this model, two important parameters must be obtained or well estimated beforehand. The two parameters are convective heat transfer coefficient of the holders in the cover zone and air leakage mass flow rate. Both of these parameters are difficult to obtain theoretically. Thus, an experimental oven and computational fluid dynamics (CFD) simulations were used to approximate them.

Furthermore, the CHT model was applied to the example production line shown in Figure 1 and numerically solved with finite difference method (FDM). Energy consumption comparison between the conventional ovens and ones with new oven design were made.

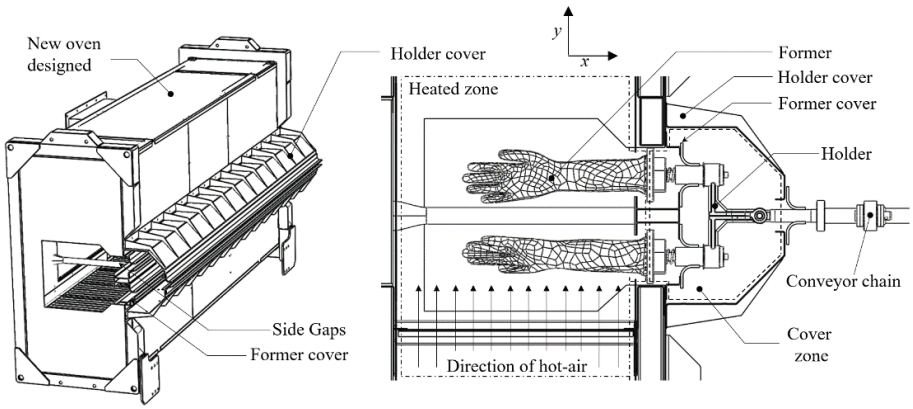

Figure 3: The components and geometries of the new oven design.

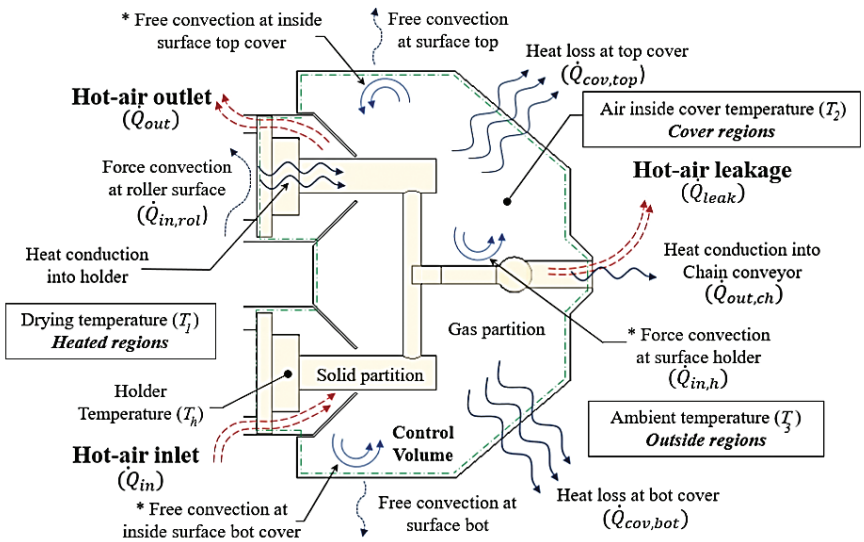

Figure 4: Heat transfer modes in the new oven design in the cover zone.

2 Problem Formulation

2.1 *Mathematical modeling*

Figure 4 shows all the heat transfers involved in the new oven design in the cover zone. Since temperature is not very high in this zone, radiation is not considered. Heat conduction out to chain conveyor can be modeled by using fin analysis. Holder temperature is a function of time but can be reasonably assumed individually uniform at any instance in time (as in lumped analysis). Transient heat equation can be applied to the control volume including both solid (holder) and gas (air) as in Equation (1) where a material derivative must be used on the left-hand side due to movement of the system and temperature gradient along the oven length (x-direction). The subscripts 1, 2, and 3 denote three separate regions in space: heated, cover and outside zones, respectively [Equation (1)].

$$\frac{D}{Dt}E_{system} = \dot{Q}_{total,h} + \dot{Q}_{total,2} \tag{1}$$

T_1 and T_3 are assumed uniform in each subprocess, while T_2 can vary in space and time. The holder temperature, T_h, can also vary in space and time. The transient heat equation can also be applied separately to holder and air in the cover zone. This results in Equations (2) and (3):

$$\frac{\partial T_h}{\partial t} + v\frac{\partial T_h}{\partial x} = \frac{\dot{Q}_{total,h}}{\rho_h c_{p,h}} \quad (2)$$

$$\frac{\partial T_2}{\partial t} = \frac{\dot{Q}_{total,2}}{\rho_2 c_{p,2}}, \quad (3)$$

where v is the conveyor speed, ρ_h is the holder density, ρ_2 is air density in the cover zone, $c_{p,h}$ is the specific heat of the holder and $c_{p,2}$ is the specific heat of the air. While the holder is moving at conveyor speed, the air in the cover zone is assumed to be have negligible mean velocity in x-direction. Thus, there is no advective term in Equation (4). The net heat transfers in and out of the two control volumes, $\dot{Q}_{total,h}$ and $\dot{Q}_{total,2}$, can be broken down further as follows:

$$\dot{Q}_{total,h} = \dot{Q}_{in,rol} + \dot{Q}_{in,h} - \dot{Q}_{out,ch} \quad (4)$$

$$\dot{Q}_{total,2} = \dot{Q}_{in} - \dot{Q}_{out} - \dot{Q}_{leak} - \dot{Q}_{in,h} - \dot{Q}_{out,h}, \quad (5)$$

where each term on the right-hand sides is as shown in Figure 4.

2.2 *Initial and Boundary Conditions*

Since the governing Equations (4) and (5) are differential equations with T_h and T_2 as functions of time and spatial coordinate x, initial and boundary conditions are required to solve for them. Note that when solving only for the steady-state solution, the initial condition is irrelevant. Also, when the path is a closed loop (as it will be when considering the entire production line), one will have a periodic boundary condition in which case no numeric value needs to be specified for the boundary conditions either.

In this work, as an intermediate step when calculating only for one subprocess (i.e. one oven), the initial holder temperature is set to be ambient temperature of 32°C and the initial cover zone air temperature is a function of the set oven temperature (T_1) based on the experiment conducted in [14]. As for boundary conditions the holder is assumed to be at 32°C when coming into the oven. Note that boundary condition for the air is not needed due to the absence of the advective term.

2.3 *FDM formulation*

Backward finite difference scheme in space and Forward Euler time advancement scheme are chosen to solve the governing Equations (2) and (3), mainly for simplicity. This results in discretized Equations (6) and (7):

$$T_h(x,t) \approx \left[\frac{\dot{Q}_{total,h}(t)}{\rho_h c_{p,h}} - v\left(\frac{T_h(x,t) - T_h(x-\Delta x,t)}{\Delta x}\right)\right]\Delta t + T_h(x,t-\Delta t) \quad (6)$$

$$T_2(x,t) \approx \left[\frac{\dot{Q}_{total,2}(t)}{\rho_2 c_{p,2}}\right]\Delta t + T_2(x,t-\Delta t), \quad (7)$$

where Δx and Δt are spatial grid size and time step, respectively. The FDM can also be used to approximate all heat flux terms in Equations (4) and (5) as shown in Table 1, where h_{rol} is the convective heat transfer coefficient of a plate between former and holder, $A_{s,rol}$ is the surface area of the plate, h_h is the convective heat transfer coefficient of a holder , $A_{s,h}$ is the surface are of a holder, $R_{wall,top}$ is the thermal resistant at top holder cover, $R_{wall,bot}$ is the thermal resistant at bot holder cover, h_f is the convective heat transfer coefficient of a conveyor chain, P is the perimeter of the conveyor chain, k_{ch} is the thermal conductivity of conveyor chain, A_{ch} is the cross section area of chain between cover and outside regions, $\dot{m}_{in}$, $\dot{m}_{out}$ and $\dot{m}_{leak}$ are the mass flow rates moving in and out of the cover region, $c_{p,1}$, $c_{p,2}$ and $c_{p,3}$ are the specific heats of air moving in, out and leak the control volume.

Table 1: Calculation of various heat flux terms

Term	Analytical Expression	FDM Approximation
$\dot{Q}_{in,rol}$	$= h_{rol}A_{s,rol}(T_1 - T_h)$	$\approx h_h A_{s,rol}(T_2(x-\Delta x) - T_h(x-\Delta x))$
$\dot{Q}_{in,h}$	$= h_h A_{s,h}(T_2 - T_h)$	$\approx h_h A_{s,h}(T_2(x-\Delta x) - T_h(x-\Delta x))$
$\dot{Q}_{cov,top}$	$= (T_2 - T_3)/R_{wall,top}$	$\approx (T_2(x-\Delta x - T_3)/R_{wall,top}$
$\dot{Q}_{cov,bot}$	$= (T_2 - T_3)/R_{wall,bot}$	$\approx (T_2(x-\Delta x - T_3)/R_{wall,bot}$
$\dot{Q}_{out,ch}$	$= (h_f k_{ch} A_{ch} P)^{1/2}(T_h - T_3)$	$\approx (h_f k_{ch} A_{ch} P)^{1/2}(T_h(x-\Delta x - T_3)$
$\dot{Q}_{in}$	$= \dot{m}_{in} c_{p,1}(T1 - T_2)$	$\approx \dot{m}_{in} c_{p,1}(T_1 - T_2(x-\Delta x))$
$\dot{Q}_{out}$	$= \dot{m}_{out} c_{p,2}(T_2 - T_1)$	$\approx \dot{m}_{out} c_{p,2}(T_2(x-\Delta x) - T_1)$
$\dot{Q}_{leak}$	$= \dot{m}_{leak} c_{p,3}(T_2 - T_3)$	$\approx \dot{m}_{leak} c_{p,3}(T_2(x-\Delta x) - T_3)$

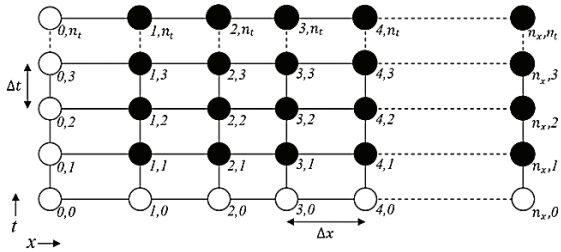

Figure 5: FDM computational domain showing unknown data nodes (black) and known data nodes (white).

There are many numerical methods to solve Equations (6) and (7). In this work, we used a simple iterative approach as shown in Figure 5. In the figure, *x*-axis is the distance along over length and *y*-axis is time. Each white node is fixed by initial or boundary condition and each black node is computed from its lower and/or left neighbor nodes. This whole process is repeated until converged.

3 Estimation of Parameters

The convective heat transfer coefficient of a holder (h_h) and the mass flow rates moving in and out of the cover region ($\dot{m}_{in}$, $\dot{m}_{out}$ and $\dot{m}_{leak}$) are important parameters for predicting the holder temperature change. Unfortunately, their accurate estimations are difficult to obtain theoretically. In this section, the experimental testing to obtain the heat transfer coefficient and the CFD simulation to obtain the mass flow rates are briefly described.

3.1 *Experimental testing*

Details of this testing oven can be found in Ref. [15]. The experimental oven with the new design was built. Figures 6 and 7 show its schematic design and actual photo. In the experiment, temperature of heat region (T_1) was set to be 140 ± 2°C by an automatic control unit. The initial temperature of holder (T_h) was 32°C. The convective heat transfer coefficient of a holder was estimated to be 6.18 W/m^2·K by using lumped analysis and curve fitting techniques.

3.2 *CFD Analysis*

CFD simulations were carried out using ANSYS Fluent

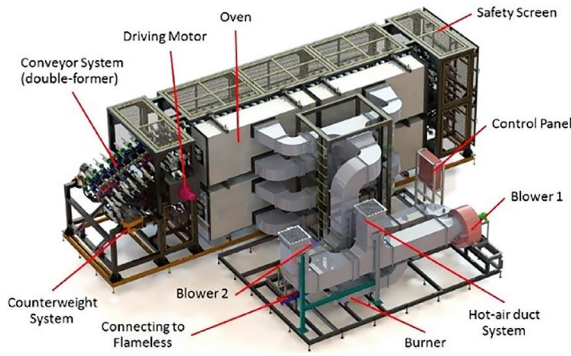

Figure 6: Schematic design of the experimental oven with the new design showing its components.

Figure 7: Experimental oven with the new design.

v15.0 with the objective to estimate mass flow rates of air in and out of the cover zone through various openings. The simulation was setup as steady and incompressible with Realizable *k*-*ε* turbulence model. Heat transfer through solid parts – including oven walls, two cover plates, a holder and a former – was also taken into account. The simulation domain includes the heated zone where hot air flowed in uniformly from the bottom boundary. This air inlet temperature was set at 90, 105, 120, and 150°C and its velocity at 0.5 m/s. Only one holder was included with periodic boundary in the moving direction. Multi-zone approach and hexahedral cells were used for meshing. The final mesh was composed of 80 zones and roughly 6.7 million cells with mesh skewness of 0.149 (Figure 8).

The oven walls consist of three layers with 50-mm fiber insulation between two 2-mm steel plates. Thermal conductivity of fiber insulation is 0.055 W/m-K and that of steel is 45 W/m-K. Each cover plate is 25-mm fiber insulation attached to a 2-mm steel plate.

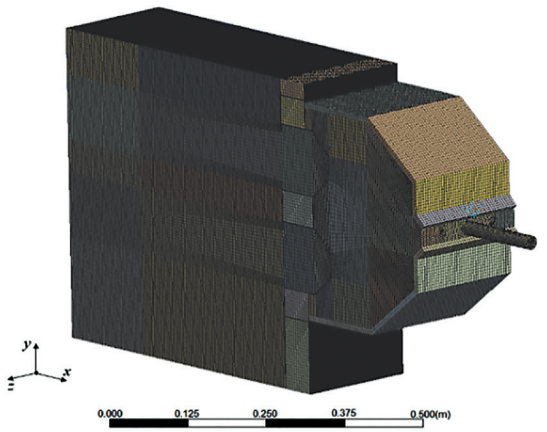

Figure 8: Mesh for the CFD simulations.

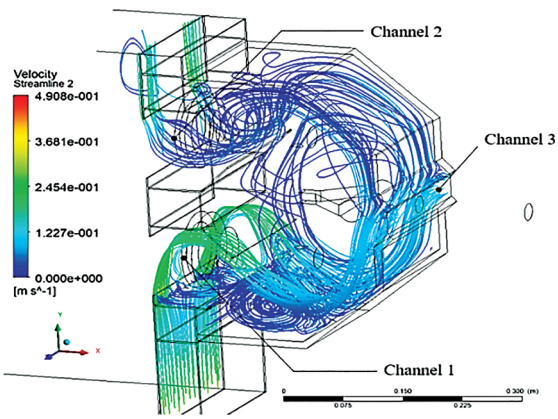

Figure 9: Air flow streamlines from the CFD results.

For different inlet temperatures, the simulations yield similar streamlines as shown in Figure 9. For 20 cm of the domain length (one holder spacing), the cover can reduce air leakage by forcing the air back into the heated zone. In addition, air velocity in the cover zone is much lower than that in the heated zone. There are air circulations at several corners inside the cover zone because of the complex geometry. The mass flow rate from the heated zone to the cover zone ($\dot{m}_{in}$) and that in the reverse direction ($\dot{m}_{out}$) are 0.0370 kg/s and 0.0364 kg/s, respectively. The leakage mass flow rate ($\dot{m}_{leak}$) is 0.0006 kg/s, which is very small, and thus its associated heat loss can be ignored.

Temperature distribution for T_1 = 150°C at the middle plane (through the holder) is shown in Figure 10. It shows that the cover is quite effective in preventing

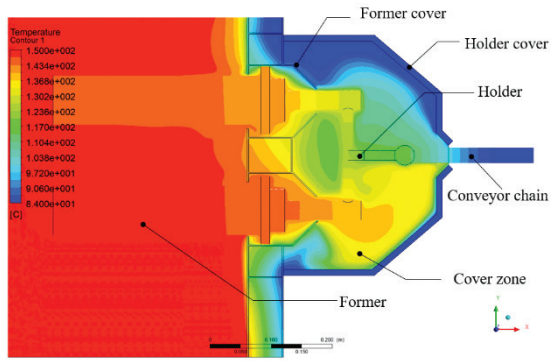

Figure 10: Air temperature distribution from the CFD results, T_1 = 150°C.

the heat loss. This shows a promising potential that an oven with outside conveyor chain can reduce the overall heat load with the conveyors. They have consistent results with testing in Ref. [15].

4 Results and Discussion

After the mass flow rates and the convective heat transfer rate were obtained, the governing Equations (7) and (8) could be solved by FDM as discussed above. Table 2 shows values of other parameters used in the calculation. Densities and specific heats are functions of temperature and standard values were employed.

Table 2: Parameter values used in the calculation

Var.	Value	Unit	Var.	Value	Unit
A_{ch}	0.245*	cm^2	h_f	6	$W/m^2{\cdot}K$
$A_{s,rol}$	155*	cm^2	h_h	6.18	$W/m^2{\cdot}K$
$A_{s,h}$	5165*	$cm^2\,cm^2$	h_{rol}	5	$W/m^2{\cdot}K$
$\dot{m}_{in}$	0.185*	kg/s	k_{ch}	54	W/m·K
$\dot{m}_{out}$	0.182*	kg/s	P	7.85	cm
$\dot{m}_{leak}$	0.003*	kg/s	$R_{wall,top}$	18.05	K/W
v	0.3	m/s	$R_{wall,bot}$	19.52	K/W

*per unit one meter of oven length

4.1 *A single oven: Coagulant drying*

As the intermediate step, the 36-m-long coagulant drying oven of 120°C was studied as verification as well as a test case. The holder was assumed to be at 30°C before entering into the oven. Various spatial grid sizes were used ranging from 0.1 to 0.0001 m.

Tables 3 and 4 show calculated results every

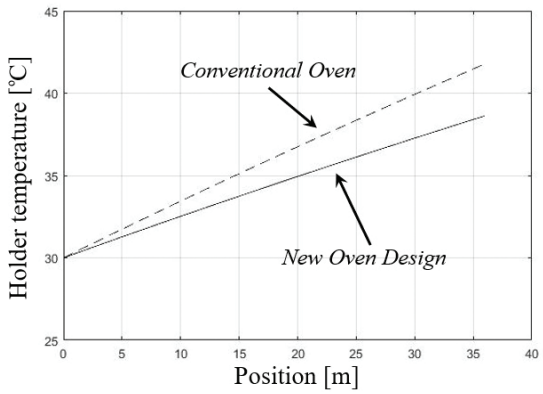

Figure 11: Comparison of holder temperature profiles (T_h) between the conventional and new oven designs.

5 m for different grid sizes. This clearly shows grid convergence. In future calculations, grid size of 0.1 m was used. In this verification test case, the error estimate for using this grid size was less than 0.006% everywhere (by comparing the computed result to that with the smallest grid size of 0.0001 m).

Figure 11 shows the holder temperature profile along the oven length by comparing the conventional oven and new oven designs. The resulting exit temperature of new oven design is smaller than that of the conventional design as expected. The difference was approximately 3°C over the length of 36 m or roughly a third of the overall temperature increase.

4.2 *The Entire Production Line*

The entire production line as specified in Figure 1 was considered for analysis. All subprocesses as well as free-chain sections were calculated as blocks, each of which the FDM approach described above was used to calculate the temperature profiles.

The initial conditions of all unknown temperature profiles are set to 30°C. The boundary conditions are connected from one subprocess to the next in a cyclic manner, thus no numeric value needs to be assigned. The unknown values were updated in the forward moving direction iteratively until the values did not change from one iteration to the next. This results in the steady-state temperature profiles of the holder for the entire line as well as the air in the cover zone of each oven. Figure 12 shows this result for the conventional oven and the new oven design.

In the production line with the conventional ovens, the average holder temperature is 76.6°C, whereas that with new oven design it is only 59.4°C. Heat loss in the production lines could also be calculated. Table 5 shows the heat loss comparison between the two designs for each of the four drying ovens (coagulant, latex, vulcanization and post). As expected, the new oven design has smaller heat losses through holder and conveyor chain, by 40% and 95%, respectively. However, the new design also has additional heat loss through the cover plates.

Table 3: Holder temperature of the conventional oven using different spatial grid sizes

Δ*x* [m]	Holder Temperature [°C] at Specified Location						
	5 m	10 m	15 m	20 m	25 m	30 m	35 m
1	31.9109	33.6130	35.2823	36.9192	38.5246	40.0989	41.6428
0.1	31.7532	33.4554	35.1248	36.7619	38.3675	39.9421	41.4864
0.01	31.7374	33.4396	35.1090	36.7462	38.3518	39.9265	41.4707
0.001	31.7359	33.4381	35.1074	36.7446	38.3502	39.9249	41.4692
0.0001	31.7357	33.4379	35.1073	36.7445	38.3501	39.9247	41.4690

Table 4: Holder temperature of the new oven design of the varied spatial grid sizes

Δx [m]	Holder Temperature [°C] at Specified Location						
	5 m	10 m	15 m	20 m	25 m	30 m	35 m
1	31.3994	32.6459	33.8683	35.0671	36.2427	37.3956	38.5262
0.1	31.2839	32.5305	33.7530	34.9519	36.1277	37.2808	38.4117
0.01	31.2724	32.5189	33.7414	34.9404	36.1162	37.2693	38.4003
0.001	31.2712	32.5178	33.7403	34.9392	36.1151	37.2682	38.3991
0.0001	31.2711	32.5176	33.7402	34.9391	36.1149	37.2681	38.3990

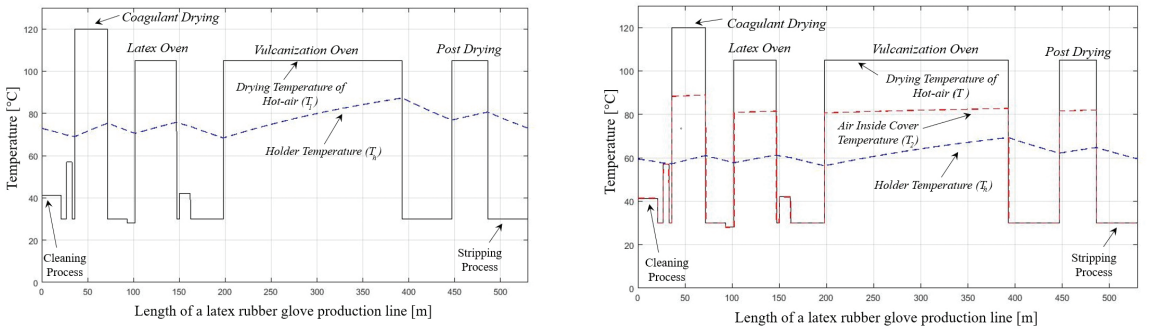

Figure 12: Comparison of temperature profiles between the conventional oven (left) and the new oven design (right) for the entire production line. The latter yields roughly 17.2°C lower in average holder temperature.

Table 5: Heat loss comparison between the conventional oven and the new oven design for each of the four drying ovens in the process

Oven	T_1 [°C]	Conventional Design				T_2 [°C]	New Oven Design				
		Heat Loss [kW]					Heat Loss [kW]				
		Holder	Chain	Walls	Total		Holder	Chain	Walls	Covers	Total
Coag. drying	120	27.25	25.46	22.26	**74.98**	85.79	16.27	0.34	22.93	6.84	**46.39**
Latex drying	105	22.64	14.97	27.83	**65.45**	75.95	13.34	0.85	28.67	6.75	**49.66**
Vulcanization	105	81.44	50.61	120.60	**252.66**	76.84	50.37	2.40	124.23	29.25	**206.25**
Post-drying	105	16.10	13.63	24.12	**53.86**	76.65	9.91	0.79	24.85	5.85	**41.39**
				Total Heat Loss	**446.94**					Total Heat Loss	**343.67**

The heat loss through oven walls are only 3% difference due to little difference in the surface areas between the two designs. The overall heat loss for the production line with the conventional ovens is 446.9 kW, while with the new oven designs it is only 343.7 kW. This accounts for 23.1% reduction in thermal waste. Assuming that the thermal energy cost is about 17.5% of the production cost, this thermal waste reduction will result in about 3.92% decrease in the production cost.

The authors would like to note that it was experimentally difficult to validate the mass flow rates obtained here from the CFD simulation. This is due to their being small values inside a geometrically complex heated oven. Therefore, a sensitivity analysis of these parameters should be performed to understand how large their impacts are on the final results. Table 6 shows the total heat loss for the entire production line and the reduction in thermal waste for scaled values of the mass flow rates, from zero up to five times the nominal values.

Table 6: Sensitivity analysis of the mass flow rates, $\dot{m}_{in}$, $\dot{m}_{out}$ and $\dot{m}_{leak}$ on the total heat loss and thermal waste reduction

Scaling Factor	Total Heat Loss [kW]	Thermal Waste Reduction [%]
0	338.54	24.25
1.0	343.69	23.10
1.5	345.77	22.64
2.0	347.58	22.23
5.0	354.47	20.69

This result shows that the mass flow rates have a relatively low impact on the thermal waste reduction. Even if the mass flow rates were to increase five folds, the new oven design would still perform better. In this case, the thermal waste reduction would only slightly change from 23.1% to 20.7%.

5 Conclusions

The concept of moving the holder and conveyor chain out of the heated zone have a good potential to reduce the heat loss in the drying process. This work formulates a mathematical model of the CHT process for the new oven design with the chain outside of the heated zone and the holder in the intermediate cover zone. FDM was then applied to solve for the unknown temperature profiles numerically. The method works for both conventional and new designs. A realistic production line was considered as an example. Experimental oven and CFD simulations were employed to estimate various mass flow rates and convective heat transfer, both of which would be difficult to obtain accurately through a theoretical estimation.

The numerical results show that the new oven design when replacing the conventional ovens can reduce the average holder temperature by 15°C and the thermal waste by 21.7% in the production line in consideration. The estimate total saving is 3.8% of the overall production cost.

Acknowledgments

This work is part of the two researches granted by Thailand Research Fund (TRF) entitled "Conceptual Design of Production Line for Advance Manufacturing of Natural Rubber Medical Glove," (Grant No. RDG5850117) and "Industrial-Scale Prototypes of an Oven and a Stripping Machine for an Advanced Manufacturing Line of Natural Rubber Medical Gloves," (Grant No. RDG5950036).

References

[1] T. Defraeye, "Advanced computational modelling for drying processes – A review," *Applied Energy*, vol. 131, no. 3, pp. 323–344, Jul. 2014.

[2] W. Jitwiriya, T. Chantrasmi, P. Yongyingsakthavorn, and U. Nontakaew, "Energy minimizing analysis for continuous drying ovens in a latex-glove production line with humidity," in *International Conference on Engineering Science and Innovative Technology*, 2016, pp. 372–379.

[3] C. Rattanapan, T. T. Suksaroj, and W. Ounsaneha, "Development of eco-efficiency indicators for rubber glove production by material flow analysis," *Procedia – Social and Behavioral Sciences*, vol. 40, pp. 99–106, Mar. 2012.

[4] A. K. Haghi, "A mathematical model of the drying process," *Acta Polytechnica*, vol. 41, no. 3, pp. 20–23, Jan. 2001.

[5] Z. Wang, J. Sun, X. Liao, F. Chen, G. Zhao, J. Wu, and X Hu, "Mathematical modeling on hot air drying of thin layer apple pomace," *Food Research International*, vol. 40, pp. 39–46, Jan. 2007.

[6] A. M. Castro, E. Y. Mayorga, and F. L. Moreno, "Mathematical modelling of convective drying of fruits: A review," *Journal of Food Engineering*, vol. 223, pp. 152–167, Apr. 2018.

[7] C. Lamnatou, E. Papanicolaou, V. Belessiotis, and N. Kyriakis, "Finite-volume modelling of heat and mass transfer during convective drying of porous bodies – Non-conjugate and conjugate formulations involving the aerodynamic effect," *Renewable Energy*, vol. 35, pp. 1391–1402, Jul. 2010.

[8] F. A. Khan and A. G. Straatman, "A conjugate fluid-porous approach to convective heat and mass transfer with application to produce drying," *Journal of Food Engineering*, vol. 179, pp. 55–67, Jun. 2016.

[9] T. Defraeye, B. Blocken, and J. Carmeliet, "Analysis of convective heat and mass transfer coefficient for convective drying of a porous flat plate by conjugate modelling," *International Journal of Heat and Mass Transfer*, vol. 55, pp. 112–124, Jan. 2012.

[10] T. Defraeye and A. Radu, "Convective drying of fruit: A deeper look at the air-material interface by conjugate modeling," *International Journal of Heat and Mass Transfer*, vol. 108, pp. 1620–1622, May. 2017.

[11] A. Dorfman and Z. Renner, "Conjugate problems in convective heat transfer: Review," *Hindawi Publishing Corporation Mathematical Problems in Engineering*, vol. 2009, pp. 1–27, 2009.

[12] G. Fedorko, V. Molnar, M. Dovica, T. Toth, and M. Kopas, "Analysis of pipe conveyor belt damaged by thermal wear," *Engineering Failure Analysis*, vol. 45, pp. 41–48, Oct. 2014.

[13] N. E. Elzayady, R. M. Rashad, M. Elgamil, and M. A. Elhabak, "Design and manufacturing of thermal cyclic fatigue apparatus," *Journal of*

American Science, vol. 8, pp. 600–606, Aug. 2012.

[14] P. Yongyingsakthavorn, T. Chantrasmi, T. Sriyubol, P. Nimdum, A. Tohsan, and U. Nontakaew, "Innovative design of latex gloves production lines via modular industrial-sized prototypes," in *IOP Conference Series: Materials Science and Engineering*, 2019, vol. 526, no. 1, pp. 1–4.

[15] W. Jitwiriya, T. Chantrasmi, P. Yongyingsakthavorn, and U. Nontakaew, "Design and energy analysis of the prototype drying oven for rubber gloves production process," in *International Conference on Engineering Science and Innovative Technology*, 2018, pp. 533–540.